Acta Cryst. (1972). B28, 3377

The Crystal Structure of Parpanit

BY E. A. H. GRIFFITH AND B. E. ROBERTSON

Division of Natural Sciences and Mathematics, University of Saskatchewan, Regina, Canada

(*Received* 30 *June* 1972)

Crystals of parpanit (panparnit, caramiphen hydrochloride, 2-diethylaminoethyl-1-phenylcyclopentanecarboxylate hydrochloride, $C_{18}H_{28}O_2NCl$) are monoclinic, space group $P2_1/c$; $a=6{\cdot}557$ (4), $b=23{\cdot}068$ (12), $c=12{\cdot}512$ (7) Å, $\beta=111{\cdot}58$ (4)°, $Z=4$, $D_m=1{\cdot}22$ (2), $D_x=1{\cdot}26$ g.cm^{-3}. The integrated intensities of 4060 independent reflexions were measured with an automated diffractometer, of which 2711 were used in the refinement. The structure was solved by direct methods and refined by full-matrix least-squares calculations to a final least-squares residual of 0·044. The ammonium proton is hydrogen bonded to the anion rather than the acyl oxygen atom, as has been inferred to be the case in solution studies. The torsional angle C–O–C–C is $\pm 170{\cdot}6°$ and the torsional angle O–C–C–N^+ is $\mp 85{\cdot}7°$.

Introduction

Some derivatives of choline are used therapeutically either as anaesthetics or to block the action of excess acetylcholine which accumulates in cholinergic systems when the hydrolytic activity of the enzyme anticholinesterase is inhibited. The conformational relationship between the choline derivative and acetylcholine is of primary importance in understanding the biochemical mechanism of the derivative. The preparation and pharmacological effectiveness of parpanit (panparnit, caramiphen hydrochloride, 2-diethylaminoethyl-1-phenylcylopentanecarboxylate hydrochloride, $C_{18}H_{28}O_2NCl$) and its analogues have been studied extensively by Bannard and coworkers (Bannard & Parkkari, 1969). Also Bannard, McCubbin & Moir (1972) have carried out a detailed investigation of the conformation of parpanit in solution. They have concluded on the basis of the n.m.r. shielding of the ethyl hydrogen atoms by ring currents, n.m.r. coupling constant data and infrared spectral information, that in solution the nitrogen atom is intramolecularly hydrogen bonded to the ester oxygen atom, which gives a *syn-periplanar* (using the notation introduced by Klyne & Prelog, 1960) conformation to the ethanolamine chain. The structure of acetylcholine and other compounds containing the ethanolamine moiety have shown the ethanolamine group to be in the *syn-clinal* conformation in the solid state (Sundaralingam, 1968). This study was undertaken at the suggestion of Bannard and coworkers in order to investigate the possible existence of an intramolecular hydrogen bond in parpanit in the solid state and to determine the conformation of the ethanolamine chain.

Experimental

A sample of parpanit was obtained from Bannard and coworkers and was easily recrystallized from acetone, giving small white crystals suitable for diffraction studies. A crystal with dimensions $0{\cdot}8\times0{\cdot}5\times0{\cdot}4$ mm was mounted on a fibre with the long axis parallel to the fibre axis, and was examined by film methods. The systematic absences ($h0l$, $l=2n+1$; $0k0$, $k=2n+1$) and Laue symmetry gave the space group $P2_1/c$. 35 reflexions between the 2θ values of 36 and 50°, where the Mo $K\alpha_1$ and Mo $K\alpha_2$ diffraction peaks were well resolved, were then centred on a Picker FACS-I automated diffractometer. These were used to calculate the cell constants by a least-squares fit using the program *PICK*2, written by W. C. Hamilton. The cell constants are given below with estimated errors given as three times the estimated standard deviations determined from the least-squares analysis.

Crystal data

$a=6{\cdot}557$ (4) Å	Space group $P2_1/c$
$b=23{\cdot}068$ (12)	$V=1760$ Å^3
$c=12{\cdot}512$ (7)	F.W. = 325·9
$\beta=111{\cdot}58$ (4)°	$Z=4$
μ(Mo $K\alpha$) = 2·34 cm^{-1}	$D_m=1{\cdot}22$ (2) g.cm^{-3} (flotation)
λ(Mo $K\alpha_1$) = 0·70926 Å	$D_x=1{\cdot}23$
$T=22$ °C	$F(000)=704$.

The angle settings of 12 of the centred reflexions were used to determine the orientation of the crystal on the diffractometer. The integrated intensities of the 4060 independent reflexions with 2θ values between 3·5 and 55° were measured in the θ–2θ scan mode. A graphite monochromator was used with a scan rate of 2·0° min^{-1} over a 3·5° base width. The background on each side of the peak was counted for 20 sec. The intensities of three standard reflexions were measured after every 100 reflexions and were not found to vary significantly. Because of the short b^* axis, reflexions with $h=0$ and low l nearly overlapped along the direction of the 2θ scan. The integrated counts for some of these reflexions were collected by hand.

The data were corrected for Lorentz and polariza-

Table 1. *Observed and calculated structure factors* ($\times 10$)

The reflexions marked with an asterisk were not used in the refinement.

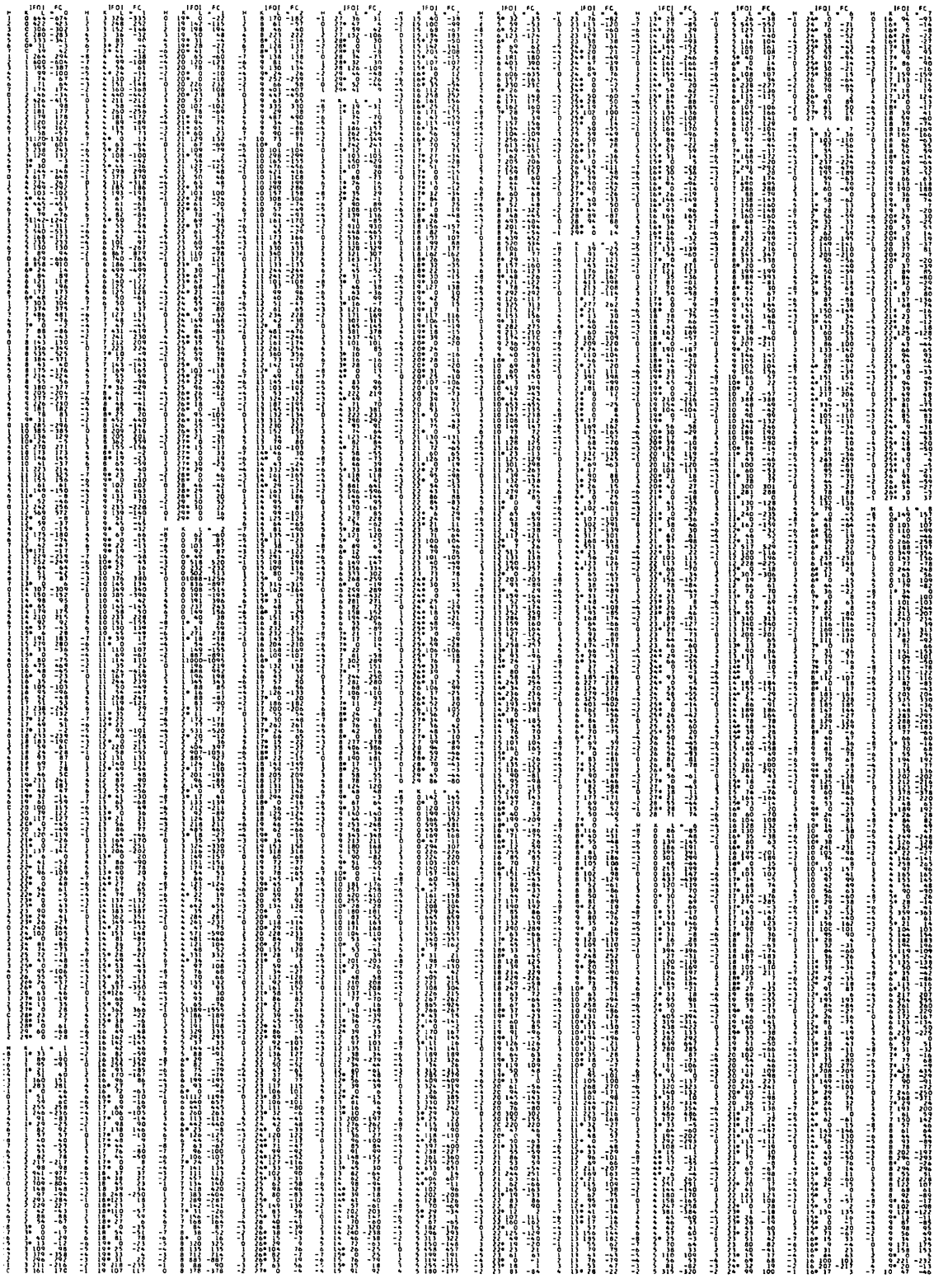

Table 1 (*cont.*)

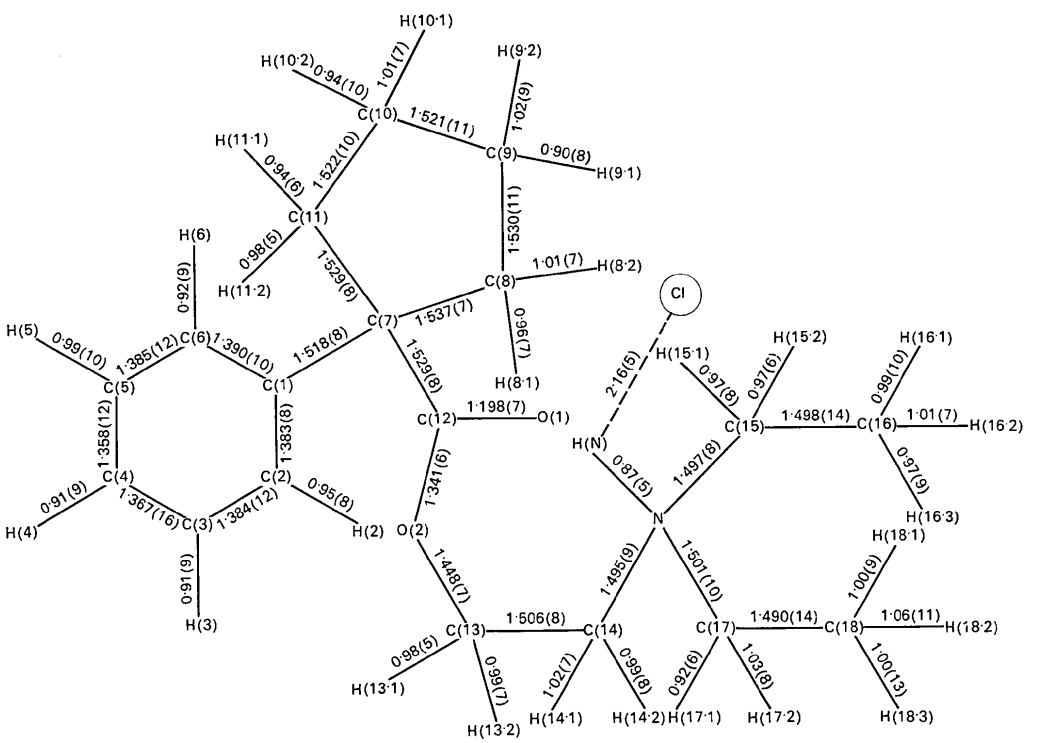

Fig. 1. Atom numbering sequence and bond lengths. The numbers in parentheses are estimated errors.

tion effects and were reduced to observed structure factors $|F_o|$, but no absorption or extinction corrections were made. The estimated error, σ, of each reflexion was calculated as $\sigma=\sigma'+1{\cdot}0+0{\cdot}10\ |F_o|$ where σ' is based on counting statistics and is given by

$$\sigma'=A\{NS+[T(NS)/T(BG)]^2BG\}^{1/2}/2\mathrm{Lp}|F_o|$$

where A is an attenuator constant, NS the number of scan counts, BG the total background count and $T(NS)$ and $T(BG)$ are the scan times and total background count times. The scattering factors of the carbon nitrogen, oxygen and chlorine atoms were those of Cromer & Mann (1968). The scattering factor for the hydrogen atoms was that given by Stewart, Davidson & Simpson (1965).

Determination and refinement of the structure

A Wilson statistical calculation was used to determine a scale factor, an overall temperature factor of 3·3 Å^2 and the normalized structure factors, E. The 387 reflexions for which $|E|>1{\cdot}73$ were used with the multiple-solution, logical symbolic addition method programs of Germain & Woolfson (1968). The set of signs with the third highest figure of merit gave a solution which showed 19 of the 22 non-hydrogen atoms. The other non-hydrogen atoms were found from a difference Fourier map and after one cycle of full matrix least-squares calculations with isotropic temperature factors, the normalized least-squares residual, R_w, was reduced to 0·126 for 1200 low angle reflexions, assuming unit weights;

$$R_w=[\sum(w||F_o|-|F_c||^2)/\sum w|F_o|^2]^{1/2}.$$

The program *FORDAP*, written by Zalkin (1965), was used for all Fourier calculations, and the program *ORFLS* written by Busing, Martin & Levy (1962) was used for full-matrix least-squares refinement. The refinement was continued with anisotropic temperature factors and R_w was reduced to 0·107. The hydrogen atoms were found from difference-Fourier maps and their positional coordinates and isotropic temperature factors were refined. All the data for which $|F_o|/\sigma>2{\cdot}30$, which numbered 2711, were used in the final cycles of refinement with the least-squares weights calculated as

$$w^{-1/2}=0{\cdot}7725-0{\cdot}04145|F_o|+0{\cdot}00110|F_o|^2.$$

The final value of both R_w and the conventional R value were both 0·044. The observed and calculated structure factors are given in Table 1.

The positional coordinates and thermal parameters are listed in Table 2, with estimated errors calculated as three times the estimated standard deviations from the least-squares analysis. The final bond lengths, bond angles and atom numbering sequence are given in Figs. 1 and 2. The equations of some of the molecular planes, the angles between them and the torsional angles of the molecule are given in Table 3. Stereoscopic views of the details of one molecule and of the molecular packing are shown in Figs. 3 and 4. These were prepared with the program *ORTEP* written by Johnson (1965).

Table 2. *Structural parameters for parpanit*

(*a*) Positional coordinates ($\times 10^4$)

	x	y	z
C(1)	5104 (10)	−5 (2)	2433 (5)
C(2)	6740 (12)	−186 (3)	3440 (6)
C(3)	8194 (15)	−621 (4)	3434 (9)
C(4)	8034 (16)	−879 (3)	2420 (9)
C(5)	6478 (14)	−700 (3)	1414 (8)
C(6)	5001 (12)	−270 (3)	1414 (7)
C(7)	3493 (9)	468 (2)	2436 (5)
C(8)	1204 (10)	408 (3)	1488 (5)
C(9)	−274 (11)	791 (4)	1897 (7)
C(10)	861 (11)	848 (3)	3196 (7)
C(11)	2909 (10)	471 (3)	3519 (5)
C(12)	4475 (8)	1046 (2)	2259 (4)
C(13)	6685 (9)	1849 (2)	3143 (5)
C(14)	8221 (9)	2028 (3)	4325 (5)
C(15)	6810 (12)	3030 (3)	4415 (6)
C(16)	8741 (17)	3310 (4)	4252 (8)
C(17)	5316 (12)	2214 (4)	5162 (6)
C(18)	5784 (19)	1688 (5)	5908 (8)
N	7285 (7)	2440 (2)	4951 (4)
O(1)	4287 (7)	1243 (2)	1340 (3)
O(2)	5649 (6)	1309 (2)	3254 (3)
Cl	1060 (3)	2536 (1)	7242 (1)

Hydrogen atom coordinates ($\times 10^3$)

	x	y	z	B (Å^2)
H(2)	688 (12)	−1 (3)	415 (6)	4 (2)
H(3)	917 (16)	−74 (4)	413 (8)	7 (2)
H(4)	899 (14)	−117 (4)	244 (7)	6 (2)
H(5)	639 (15)	−89 (4)	68 (8)	7 (2)
H(6)	403 (12)	−12 (3)	73 (7)	5 (2)
H(8,1)	80 (11)	1 (3)	148 (6)	4 (2)
H(8,2)	111 (11)	52 (3)	70 (5)	4 (2)
H(9,1)	−160 (13)	63 (3)	170 (7)	6 (2)
H(9,2)	−35 (14)	121 (4)	159 (7)	6 (2)
H(10,1)	131 (12)	126 (3)	340 (6)	5 (2)
H(10,2)	−5 (13)	73 (3)	359 (6)	5 (2)
H(11,1)	265 (10)	8 (3)	366 (5)	3 (2)
H(11,2)	407 (10)	61 (3)	422 (5)	3 (2)
H(13,1)	553 (9)	213 (2)	276 (5)	2 (2)
H(13,2)	752 (9)	178 (3)	263 (5)	3 (2)
H(14,1)	870 (11)	167 (3)	483 (6)	4 (2)
H(14,2)	952 (11)	223 (3)	427 (5)	4 (2)
H(15,1)	641 (11)	326 (3)	495 (6)	4 (2)
H(15,2)	555 (12)	298 (3)	371 (6)	4 (2)
H(16,1)	911 (14)	310 (4)	366 (8)	6 (2)
H(16,2)	10 (14)	329 (3)	497 (8)	5 (2)
H(16,3)	836 (14)	371 (4)	402 (7)	6 (2)
H(17,1)	424 (12)	215 (3)	445 (6)	4 (2)
H(17,2)	488 (12)	255 (3)	558 (6)	4 (2)
H(18,1)	711 (17)	175 (4)	662 (9)	8 (3)
H(18,2)	617 (16)	133 (4)	548 (8)	7 (2)
H(18,3)	443 (19)	161 (5)	607 (5)	10 (3)
H(N)	834 (10)	250 (3)	561 (5)	3 (2)

Table 2 (*cont.*)

(*b*) Thermal parameters ($\times 10^3$)

The temperature factor expression for the non-hydrogen atoms is: $\exp[-2\pi^2(h^2a^{*2}U_{11}+\ldots 2hka^*b^*U_{12}\ldots.)]$.

	U_{11}	U_{22}	U_{33}	U_{12}	U_{13}	U_{23}
C(1)	38 (3)	27 (3)	41 (3)	−8 (2)	22 (2)	−4 (2)
C(2)	55 (4)	46 (4)	49 (4)	9 (3)	25 (3)	7 (3)
C(3)	67 (5)	60 (5)	81 (6)	25 (4)	37 (5)	29 (5)
C(4)	75 (6)	40 (4)	113 (8)	16 (4)	61 (6)	9 (5)
C(5)	73 (5)	43 (4)	86 (6)	−12 (4)	52 (5)	−23 (4)
C(6)	51 (4)	43 (4)	53 (4)	−7 (3)	26 (3)	−14 (3)
C(7)	31 (3)	31 (3)	32 (3)	−5 (2)	15 (2)	−4 (2)
C(8)	35 (3)	44 (4)	45 (3)	−10 (3)	12 (3)	−6 (3)
C(9)	35 (5)	66 (5)	67 (5)	2 (3)	22 (3)	1 (4)
C(10)	47 (4)	52 (4)	65 (4)	0 (3)	35 (4)	−3 (3)
C(11)	45 (3)	36 (3)	40 (3)	−6 (3)	25 (3)	−2 (3)
C(12)	26 (3)	30 (3)	32 (3)	1 (2)	13 (2)	−4 (2)
C(13)	36 (3)	29 (3)	37 (3)	−4 (2)	14 (2)	−2 (2)
C(14)	27 (3)	35 (3)	44 (3)	0 (2)	7 (2)	−5 (3)
C(15)	54 (4)	40 (4)	40 (4)	7 (3)	7 (3)	−8 (3)
C(16)	85 (6)	40 (4)	56 (5)	−6 (4)	30 (4)	−2 (4)
C(17)	39 (6)	85 (6)	40 (4)	−15 (4)	13 (3)	−12 (4)
C(18)	80 (6)	101 (8)	51 (5)	−40 (6)	21 (5)	−2 (5)
N	30 (2)	43 (3)	29 (2)	−2 (2)	4 (2)	−5 (2)
O(1)	49 (2)	45 (2)	31 (2)	−10 (2)	16 (2)	0 (2)
O(2)	37 (2)	32 (2)	31 (2)	−9 (2)	12 (2)	−4 (2)
Cl	35 (1)	52 (1)	38 (1)	−4 (1)	0 (1)	0 (1)

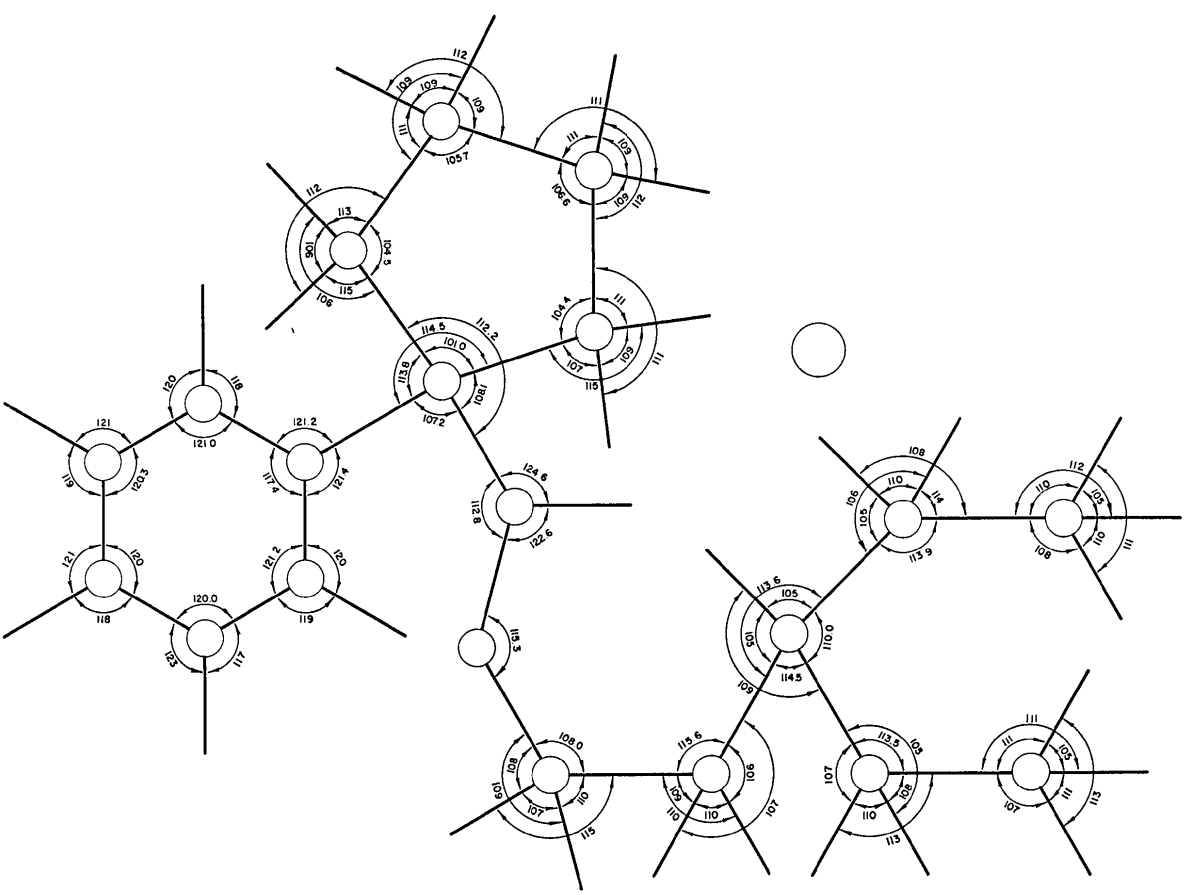

Fig. 2. Bond angles. The error in an angle not involving a hydrogen atom is *ca.* 1·2° and the error in an angle involving a hydrogen atom is *ca.* 10°.

Discussion

The molecule is involved in no unusually short contacts other than a hydrogen bond to the anion, and the conformation should be reasonably unaffected by the molecular packing. The shortest non-bonded intermolecular contact is between ethyl hydrogen atoms on adjacent molecules and has the length 2·42 Å. The structure contains only one intermolecular contact which is less than 2·80 Å in length and also involves a non-hydrogen atom, this being the 2·53 Å separation between the carbonyl oxygen atom, O(1), and an aromatic hydrogen atom, H(5), on a molecule related to the first by the translation $-\mathbf{a}$ combined with an inversion through the centre of symmetry at the origin. Short non-bonded intermolecular contacts between carbonyl oxygen atoms and aromatic hydrogen atoms are not unusual with distances as short as 2·36 Å having been reported (Guttormson & Robertson, 1972). The non-bonded contacts between two non-hydrogen atoms are all greater than 3·5 Å in length. The atom N(2) is involved in a strong hydrogen bond to the anion, with a N^+–Cl^- distance of 3·023 (4) Å. The Cl^-–H distance is 2·16 (5) Å and the angle subtended at the hydrogen atom is 174°.

The O–C–C–N^+ moiety has the torsional angle $\mp$85·7° which is the *syn-clinal* conformation. Most molecules containing this group show the *syn-clinal* conformation with torsional angles ranging from 50 to 90°. (Sundaralingam, 1968; Chothia & Pauling, 1969; Beall, Herdklotz & Sass, 1970). Kier (1967) used

Table 3. *Molecular planes and torsional angles*

(*a*) Equations of planes $Ax+By+Cz=D$. Coordinates refer to the directions of the *a*, *b* and *c** axes.

Plane	*A*	*B*	*C*	*D*
I	0·7167	0·6876	−0·1167	1·2642
II	−0·0722	0·9958	−0·0556	0·8319
III	0·5917	0·7994	−0·1048	0·6210
IV	−0·8759	0·4817	−0·0277	−0·5801
V	−0·7694	−0·2959	−0·5662	−6·8394
VI	0·0707	−0·4122	−0·9083	−7·3616

(*b*) Dihedral angles.

Planes	Angle
I × II	50·2°
II × III	40·6
I × III	9·6
II × IV	57·0
III × IV	82·5

(*c*) Torsional angles

Bond	Angle
C(12)–O(2)	± 178·6°
O(2)–C(13)	∓ 170·6
C(13)–C(14)	∓ 85·7
C(14)–N[C(15)]	∓ 67·6
C(14)–N[C(17)]	± 60·0
N——C(15)	∓ 54·4
N——C(17)	± 62·6

Table 3 (*cont.*)

(*d*) Distances to planes. Atoms defining the plane are marked with an asterisk.

Atoms	Planes I	II	III	IV	V
C(1)	0·007*				
C(2)	−0·006*				
C(3)	−0·002*				
C(4)	0·011*				
C(5)	−0·010*				
C(6)	0·001*				
C(7)	0·015	0*	−0·636	0·003*	
C(8)		0*	−0·011*		
C(9)			0·017*		
C(10)			−0·017*		
C(11)		0*	0·010*		
C(12)				−0·010*	
C(13)				0·039	
C(14)				0·284	
O(1)				0·004*	
O(2)				0·003*	
C(15)					0·030*
C(16)					0·055*
C(17)					0·041*
C(18)					0·090*
N					−0·133*

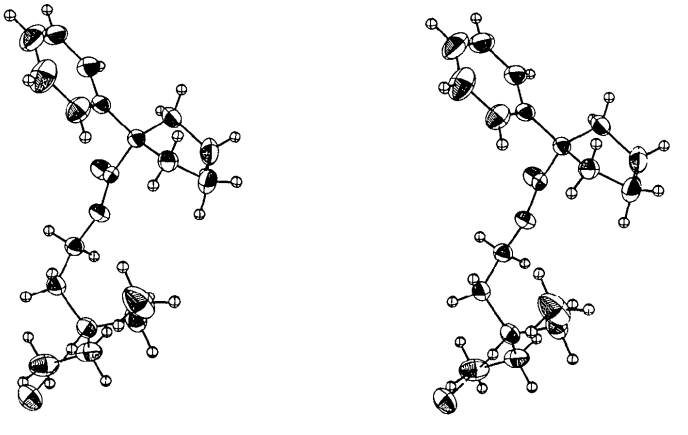

Fig. 3. Stereogram of the molecule. The hydrogen bond to the chloride ion is shown as a dotted line. The thermal ellipsoids of the non-hydrogen atoms are drawn at the limits of 50% probability.

molecular-orbital calculations to rationalize the *syn-clinal* conformation in acetylcholine, which has been observed in the solid state by Canepa, Pauling & Sörum (1966). Further, Culvenor & Ham (1966) have predicted the *syn-clinal* conformation for acetylcholine in solution on the basis of their study of n.m.r. coupling constants. Sundaralingam (1968) has suggested that this conformation is stabilized by electrostatic attraction between the positively charged nitrogen and the electronegative ester oxygen atom. The N^+–O distance of 3·279 (6) Å is representative of such distances (Beall, Herdklotz & Sass, 1970) and the distances to the nearest ethyl carbon atoms C(17)–O(2) and C(18)–O(2) are 3·232 (9) and 3·395 (12) Å respectively.

It would therefore seem reasonable to expect that the conformation observed here, or one similar to it, should be present in solution, which is in conflict with the evidence obtained by Bannard *et al.* (1972) for the presence of a conformation with an intramolecular hydrogen bond. The molecule in solution may show an equilibrium between the *syn-clinal* and the *syn-periplanar* conformations.

The torsional angle about the ester bond C(O)–O–C–C, is *anti-periplanar* as are most mimics of acetylcholine (Chothia & Pauling, 1969; Beall, Herdklotz & Sass, 1970). The only crystallographic structure determination of acetylcholine itself (Canepa, Pauling & Sörum, 1966), however, has shown a *syn-clinal* torsional angle about this bond, which is not the usual conformation of a primary ester (Mathieson, 1965). Chothia & Pauling (1970) have argued that the *syn-clinal* conformation observed in the solid state is an artifact of the molecular packing and the active conformation of acetycholine in solution is *anti-periplanar*. If this is the case, then the conformation observed here for parpanit is that of the active conformation of acetylcholine.

The mechanism of biologically active mimics of acetylcholine, either as local anaesthetics or in the treatment of anticholinesterase poisoning, may be related to a competition between the mimic and acetylcholine for the receptor sites in the synaptic gap. Receptor sites for acetylcholine are divided into *muscarinic* for which muscarine and compounds related to muscarine show specific activity and *nicotinic* for which nicotine and compounds related to nicotine show specific activity. Pharmacological studies of parpanit have not shown the relative importance of nicotinic and muscarinic receptor sites in its biological activity. Chothia (1970) has concluded from a study of the common features of muscarinic and nicotinic mimics of acetylcholine, that the side of the molecule containing the equivalent of the methyl carbon of acetylcholine must be free of additional blocking atoms beyond those present in acetylcholine in order for the mimic to show muscarinic behaviour. Also he concluded that the side of the molecule containing the carbonyl oxygen atom must be free of additional blocking atoms in order for the mimic to show nicotinic behaviour. From these considerations and the conformation of the molecule as shown in Fig. 3, we would conclude that parpanit should show nicotinic activity, which is consistent with the observation that it is particularly effective when used as an adjunct to atropine sulphate which shows muscarinic activity (Coleman, Little & Bannard, 1962).

The authors acknowledge the support of the National Research Council of Canada through research grants.

References

BANNARD, R. A. B., MCCUBBIN, A. & MOIR, R. Y. (1972). Private communication.

BANNARD, R. A. B. & PARKKARI, J. H. (1969). *Canad. J. Chem.* **48**, 1377.

BEALL, R., HERDKLOTZ, J. & SASS, R. L. (1970). *Biochem. Biophys. Res. Commun.* **39**, 329.

BUSING, W. R., MARTIN, K. O. & LEVY, H. A. (1962). *ORFLS.* Report ORNL-TM-305, Oak Ridge National Laboratory, Oak Ridge, Tennessee.

CANEPA, F. G., PAULING, P. J. & SÖRUM, H. (1966). *Nature, Lond.* **210**, 907.

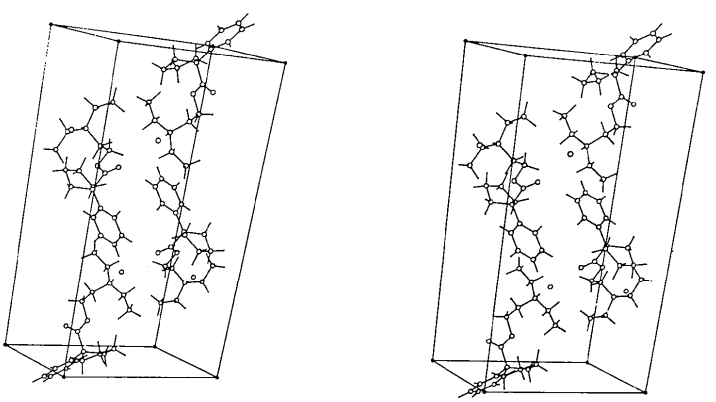

Fig4. Stereogram of the molecular packing. The origin is in the lower front left corner. The *a* axis points back into the page; the *b* axis points up; the *c* axis points to the right.

CHOTHIA, C. (1970). *Nature, Lond.* **225**, 36.
CHOTHIA, C. & PAULING, P. (1969). *Nature, Lond.* **223**, 919.
CHOTHIA, C. & PAULING, P. (1970). *Proc. Natl. Acad. Sci. U.S.* **65**, 477.
COLEMAN, L. W., LITTLE, O. E. & BANNARD, R. A. B. (1962). *Canad. J. Biochem. Physiol.* **40**, 815.
CROMER, D. T. & MANN, J. B. (1968). *Acta Cryst.* A**24**, 321.
CULVENOR, C. C. J. & HAM, N. S. (1966). *Chem. Commun.* p. 537.
GERMAIN, G. & WOOLFSON, M. M. (1968). *Acta Cryst.* B**24**, 91.
GUTTORMSON, R. & ROBERTSON, B. (1972). *Acta Cryst.* B**28**, 2702.
JOHNSON, C. K. (1965). *ORTEP.* Report ORNL-3794, Oak Ridge National Laboratory, Oak Ridge, Tennessee.
KIER, L. B. (1967). *Mol. Pharmacol.* **3**, 487.
KLYNE, W. & PRELOG, V. (1960). *Experientia*, **16**, 521.
MATHIESON, A. M. (1965). *Tetrahedron Lett.* p. 4137.
SUNDARALINGAM. M. (1968). *Nature, Lond.* **217**, 35.
STEWART, R. F., DAVIDSON, E. R. & SIMPSON, W. T. (1965). *J. Chem. Phys.* **42**, 3175.
ZALKIN, A. (1965). *FORDAP.* A Fortran Program for Fourier Calculations, Univ. of California, Berkeley.

Acta Cryst. (1972). B**28**, 3384

The Classification of Tilted Octahedra in Perovskites

BY A. M. GLAZER

Crystallographic Laboratory, Cavendish Laboratory, Cambridge, England

(*Received* 4 *May* 1972)

A simple method for describing and classifying octahedral tilting in perovskites is given and it is shown how the tilts are related to the unit-cell geometries. Several examples from the literature are listed and predictions about hitherto unknown structures of some materials are made.

Introduction

The perovskite structure is very commonly found in compounds of general formula ABX_3 and many of these materials have interesting and important properties, such as ferroelectricity, piezoelectricity, non-linear optical behaviour and so on.

Fig. 1 shows the basic unit, which consists of corner-linked octahedra of X anions (usually oxygen or fluorine) with B cations at their centres and A cations between them; the cations have been left out of the diagram since, in this paper, only the octahedra will be considered. The ideal structure thus depicted is found in some materials, for example $SrTiO_3$ at room temperature; more usually the structure is modified by cation displacements as in $BaTiO_3$, or by the tilting of octahedra as in $CaTiO_3$, or by a combination of both as in $NaNbO_3(P)$. The cation displacements, which are directly linked with ferroelectricity and antiferroelectricity, are relatively simple to deal with and in any case do not directly affect the lattice parameters except by a relatively small distortion of the octahedra. The tilting of the octahedra has usually a far greater effect on lattice parameters but is more difficult to describe. However, attempts have been made to discuss these phenomena (Megaw, 1966, 1969) and it is as a result of these studies that the present work has evolved.* It is the aim of this paper to show how the various tilt systems may be classified and how they affect the crystal symmetries. Displacements of cations are not discussed here at any length. The derived results are based on the assumption that the octahedra are regular throughout. Very commonly the overall symmetry follows that of the tilts in spite of displacements and distortions; and even when it does not, the symmetry due to the tilts can be considered separately.

This classification has already proved useful in a recent study of the $T_2 \rightarrow$ cubic transition in $NaNbO_3$ (Glazer & Megaw, 1972), in which it readily suggested a likely model for the T_2 structure. More recently, it has also been successfully used in studying the $T_1 \rightarrow T_2$ transition (Ahtee, Glazer & Megaw, 1972). In connexion with phase transitions, dynamic (as opposed to static) tilting of octahedra can be interpreted in terms of lattice modes. In fact, it seems probable that the most obvious tilt configurations generally correspond to some of the most important modes associated with phase transitions in perovskites. The present classification should therefore find some use in the lattice dynamical studies of these transitions.

Effect of octahedral tilts

When an octahedron in the perovskite structure is tilted in some particular way it causes tilting of the neighbouring octahedra. However, it is, in practice, extremely difficult to visualize the total effect, and in

* A scheme very similar to the one described here has recently been derived independently by J. K. Brandon (private communication) in connexion with the structure of $Ca_2Nb_2O_7$.